Radical Cation Ester Cleavage in Solution. Mechanism of the Mesolytic O−CO Bond Scission†

Michael Schmittel,*[,‡] Karl Peters,[§] Eva-Maria Peters,[§] Andreas Haeuseler,[‡] and Holger Trenkle[||]

FB 8 - OC1 (Chemie-Biologie) der Universität-GH Siegen, Adolf-Reichwein-Strasse, D-57068 Siegen, Germany, Max-Planck-Institut für Festkörperforschung, Heisenbergstr. 1, D-70506 Stuttgart, Germany, and Institut für Organische Chemie der Universität Würzburg, Am Hubland, D-97074 Würzburg, Germany

schmittel@chemie.uni-siegen.de

Received October 31, 2000

A wide range of enol carbonate, carbamate, and ester radical cations is characterized in solution by cyclic voltammetry and EPR spectroscopy. Preparative transformations using one-electron oxidants or anodic oxidation yield benzofurans after O−CO bond cleavage. Mechanistic investigations and direct detection of radical intermediates reveal that all enol radical cations undergo exclusively O−CO bond cleavage to provide α-carbonyl cations and acyl (or alternatively, alkoxyacyl and aminoacyl) radicals, respectively. The kinetics of the mesolytic fragmentation and the influence of nucleophilic additives have been determined using fast-scan cyclic voltammetry.

Introduction

Homolytic and heterolytic bond dissociation processes are rather well understood and have contributed in a fundamental way to our present understanding of organic chemistry. In contrast, much less is known about the thermochemistry and in particular the kinetics of bond cleavage processes of radical ions, although bond cleavage in odd-electron species[1] has become very important in synthetically useful reactions.[2]

Radical cations of almost any organic substrate can be conveniently prepared through chemical, anodic, or photochemical one-electron oxidation, and hence, it would be desirable to understand the thermodynamic and kinetic aspects of their bond cleavage pathways in solution. While at present there is extensive data available on C−H,[3] C−C,[4] and C−Si[4l,5] bond cleavage, other processes have hardly been investigated, e.g., C−O[6] and C−N[7] bond scissions and equally those involving two heteroatoms, such as O−Si (e.g., enol and phenol silyl ethers),[8] O−Sn,[9] O−Al,[10] O−P,[11] O−Ti,[12] and O−Zr.[13]

Because of the importance of ester cleavage in organic chemistry occurring along the traditional heterolytic pathways, we have recently started to investigate the O−C(=O) bond cleavage in ester radical cations,[6] a process basically unknown in solution[14] and gas-phase oxidations.[15] But how can one devise a system that undergoes clean O−C(=O) scission? It is obvious that oxidation of a pure σ (O−C) donor will lead to rather efficient bond weakening, but simple esters usually have a HOMO with high n character. Hence, we have to construct a system whose π (or n) HOMO shows some sizable overlap with the σ (O−C) orbital. While such systems may undergo efficient bond cleavage when the

† This paper is dedicated to Prof. S. Hünig on the occasion of his 80th birthday.

‡ Universität-GH Siegen.

§ Max-Planck-Institut für Festkörperforschung.

|| Universität Würzburg.

(1) Schmittel, M.; Ghorai, M. K. *Electron Transfer in Chemistry*; Balzani, V., Ed.; Wiley-VCH: Weinheim, 2001; Vol. 2, Chapter 2.1.1.

(2) Linker, T.; Schmittel, M. *Radikale und Radikalionen in der Organischen Synthese*; Wiley-VCH: Weinheim, 1998. Mella, M.; Fagnoni, M.; Freccero, M.; Fasani, E.; Albini, A. *Chem. Soc. Rev.* **1998**, *27*, 81.

(3) (a) Shaefer, C. G.; Peters, K. S. *J. Am. Chem. Soc.* **1980**, *102*, 7566. (b) Sinha, A.; Bruice, T. C. *J. Am. Chem. Soc.* **1984**, *106*, 7291. (c) Das, S.; von Sonntag, C. *Z. Naturforsch.* **1986**, *41b*, 505. (d) Lewis, F. D. *Acc. Chem. Res.* **1986**, *19*, 401. (e) Bordwell, F. G.; Cheng, J.-P.; Bausch, M. J. *J. Am. Chem. Soc.* **1988**, *110*, 2872. (f) Bordwell, F. G.; Cheng, J.-P. *J. Am. Chem. Soc.* **1989**, *111*, 1792. (g) Dinnocenzo, J. P.; Banach, T. E. *J. Am. Chem. Soc.* **1989**, *111*, 8646. (h) Hapiot, P.; Moiroux, J.; Savéant, J.-M. *J. Am. Chem. Soc.* **1990**, *112*, 1337. (i) Xu, W.; Mariano, P. S. *J. Am. Chem. Soc.* **1991**, *113*, 1431. (k) Xu, W.; Zhang, X.-M.; Mariano, P. S. *J. Am. Chem. Soc.* **1991**, *113*, 8863. (l) Anne, A.; Hapiot, P.; Moiroux, J.; Neta, P.; Savéant, J.-M. *J. Phys. Chem.* **1991**, *95*, 2370. (m) Tripathi, G. N. R. *Chem. Phys. Lett.* **1992**, *199*, 409. (n) Anne, A.; Hapiot, P.; Moiroux, J.; Neta, P.; Savéant, J.-M. *J. Am. Chem. Soc.* **1992**, *112*, 4694. (o) Bordwell, F. G.; Satish, A. V. *J. Am. Chem. Soc.* **1992**, *114*, 10173. (p) Baciocchi, E.; Del Giacco, T.; Elisei, F. *J. Am. Chem. Soc.* **1993**, *115*, 12290. (q) Goez, M.; Sartorius, I. *J. Am. Chem. Soc.* **1993**, *115*, 11123. (r) Goez, M.; Sartorius, I. *Chem. Ber.* **1994**, *127*, 2273. (s) Brede, O.; Beckert, D.; Windolph, C.; Göttinger, H. A. *J. Phys. Chem. A* **1998**, *102*, 1457. (t) Bietti, M.; Baciocchi, E.; Steenken, S. *J. Phys. Chem. A* **1998**, *102*, 7337. (u) Parker, V. D.; Zhao, Y. X.; Lu, Y.; Zheng, G. *J. Am. Chem. Soc.* **1998**, *120*, 12720. (v) Zhao, C. X.; Gong, Y. F.; He, H. Y.; Jiang, X. K. *J. Phys. Org. Chem.* **1999**, *12*, 688. (w) Baciocchi, E.; Bietti, M.; Steenken, S. *Chem. Eur. J.* **1999**, *5*, 1785.

(4) (a) Gassman, P. G.; Yamaguchi, R.; Koser, G. F. *J. Org. Chem.* **1978**, *43*, 4392. (b) Penn, J. H.; Deng, D.-L.; Chai, K.-J. *Tetrahedron Lett.* **1988**, *29*, 3635. (c) Penn, J. H.; Deng, D.-L.; Chai, K.-J. *Tetrahedron Lett.* **1988**, *29*, 3635. (d) Arnold, D. R.; Lamont, L. J. *Can. J. Chem.* **1989**, *67*, 2119. (e) Popielarz, R.; Arnold, D. R. *J. Am. Chem. Soc.* **1990**, *112*, 3068. (f) Camaioni, D. M. *J. Am. Chem. Soc.* **1990**, *112*, 9475. (g) Arnold, D. R.; Lamont, L. J.; Perrott, A. L. *Can. J. Chem.* **1991**, *69*, 225. (h) Perrier, S.; Sankararaman, S.; Kochi, J. K. *J. Chem. Soc., Perkin Trans. 2* **1993**, 825. Lucia, L. A.; Burton, R. D.; Schanze, K. S. *J. Phys. Chem.* **1993**, *97*, 9078. (i) Leon, J. W.; Whitten, D. G. *J. Am. Chem. Soc.* **1993**, *115*, 8038. (k) Maslak, P.; Vallombroso, T. M.; Chapman, Jr., W. H.; Narvaez, J. N. *Angew. Chem.* **1994**, *106*, 110−113; *Angew. Chem., Int. Ed. Engl.* **1994**, *33*, 73−75. (l) Su, Z.; Mariano, P. S.; Falvey, D. E.; Yoon, U. C.; Oh, S. W. *J. Am. Chem. Soc.* **1998**, *120*, 10676. (m) Adam, W.; Heidenfelder, T. *Chem. Soc. Rev.* **1999**, *28*, 359.

(5) Dinnocenzo, J. P.; Farid, S.; Goodman, J. L.; Gould, I. R.; Todd, W. P.; Mattes, S. L. *J. Am. Chem. Soc.* **1989**, *111*, 8973. Todd, W. P.; Dinnocenzo, J. P.; Farid, S.; Goodman, J. L.; Gould, A. L. *Tetrahedron Lett.* **1993**, *34*, 2863. Zhang, X.; Yeh, S.-R.; Hong, S.; Freccero, M.; Albini, A.; Falvey, D. E.; Mariano, P. S. *J. Am. Chem. Soc.* **1994**, *116*, 4211. Borosky, G. L.; Pierini, A. B. *THEOCHEM* **1999**, *466*, 165.

10.1021/jo0057093 CCC: $20.00
Published on Web 04/21/2001

mesolytic[16] bond strength is low, they will get involved in reactions typical of π (or n) radical cations once the mesolytic O−C(=O) bond strength is high. To avoid the latter processes, we have decided to study radical cations derived from 2,2-dimesitylenol esters, as the steric shielding of the two bulky mesityl groups effectively prevents disturbing side reactions, such as deprotonation in β-position and nucleophilic attack at the unsaturated system. This approach was successfully used to monitor slow mesolytic processes, as in O−P[11] and O−Ti[12] bond cleavage. Moreover, this approach worked for enol acetate[6] and enol trifluoroacetate[17] radical cations providing the first indication of a clean ester cleavage. In this paper, we now wish to present a comprehensive study[18] on the mesolytic O−CO bond scission in various radical cations including electron-poor as well as electron-rich esters, carbonates, and carbamates establishing such a process as a general reaction pathway as opposed to the acid and base-catalyzed ester cleavage. In addition, we have examined two bisenol ester derivatives to evaluate the concept for multibond cleavage processes.

Results

Synthesis and Characterization of the Model Compounds. To properly measure the kinetics of O−CO mesolytic cleavage, we synthesized ester systems derived from 2,2-dimesitylenols, for reasons outlined above.[8b,19a] For comparison, we have included data for **1g**,**h** and **2g**,**h**.[6,17] All systems offer decisive advantages from a practical point of view. They are oxidized at rather low potentials because of the electron-rich dimesitylenol moiety, and the products formed after O−C bond cleavage are well-known.

The enol ester derivatives **1a**−**f**, **2a**,**b**, and **3a**,**b** (Table 1) could be easily prepared by reaction of the corresponding lithium or sodium enolates with suitable acylation reagents, such as the corresponding isocyanates, anhydrides, or acyl chlorides. In most cases, yields were not too high because of the steric shielding about the OH group. The steric hindrance in the model compounds is apparent from the ^{1}H NMR spectra that exhibit significant peak broadening because of coalescence. Such a behavior has been observed in many related systems caused by a two- or three blade propeller conformation in which rotation of the mesityl groups is hindered.[19b,20] In the bisenol carbonate **3a**, the rotation is completely frozen on the time scale of the NMR experiment, and thus, a double set of signals is obtained for the *o*-mes-CH_3 and the *m*-mes-H protons.

Table 1

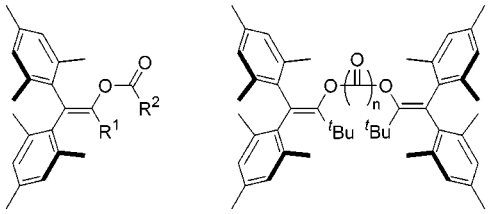

1a-h, 2a-h n = 1: **3a** (50%), n = 2: **3b** (67%)

	R^1	R^2	yield (%)		R^1	R^2	yield (%)
1a	Bu^t	NH-Bu^t	38	**2a**	Ph	NH-Bu^t	69
1b	Bu^t	O-Bu^t	25	**2b**	Ph	O-Bu^t	73
1c	Bu^t	O-CH_2Ph	11				
1d	Bu^t	*p*-An	63				
1e	Bu^t	*p*-PhN$(CH_3)_2$	43				
1f	Bu^t	Fc	31				
1g	Bu^t	CH_3	62[6]	**2g**	Ph	CH_3	77[6]
1h	Bu^t	CF_3	77[17]	**2h**	Ph	CF_3	80[17]

The X-ray analysis of **1a** ($P2_1/c$, a = 806.6(1) pm, b = 2297.1(2) pm, c = 1390.9(1) pm, β = 92.630°) and **1b** ($Fdd2$, a = 3483.4(2) pm, b = 3660.7(2) pm, c = 835.0(1) pm) uncovers the steric bulk caused mainly by the mesityl groups (Figure 1). Both mesityl rings are severely twisted out of the C=C−O plane by dihedral angles φ_1 = 59.5−62.5° (cis to OCOR) and φ_2 = 63.5−65.0°. This leads to a very efficient shielding of the β-carbons of the enol moiety thereby preventing any attack on the stage of the radical cation at this position. The situation for **1g**[21] and **1h**[22] (see Table 2) and for the corresponding simple enol (φ_1 = 66.0, φ_2 = 63.7)[23] is very similar. The C=C and C−O bond lengths are within the expected magnitude.[21−23] Interestingly, the dihedral angles for C=C−O−C are about 70° for **1a**,**b** and about 77° for **1g**,**h**, thus allowing for convenient overlap of the scissile O−CO bond with the enol π system.

One-Electron Oxidation. Preparative one-electron oxidation of the carbamates **1a**,**2a**, carbonates **1b**,**2b**, and enol esters **1d**−**e** by tris(1,10-phenanthroline)iron(III)-hexafluorophosphate ($[Fe(phen)_3]^{3+}$, $E_{1/2}$ = 0.76 V_{Fc}[24]) or thianthrenium perchlorate (TPC, $E_{1/2}$ = 0.95 V_{Fc}[24]) in acetonitrile provided the benzofuran **B1** or **B2** as the exclusive product (Scheme 1, Table 3).[25] Only in the case of enol ester **1f**, containing a ferrocene unit, conversion

(6) Schmittel, M.; Heinze, J.; Trenkle, H. *J. Org. Chem.* **1995**, *60*, 2726.
(7) Adam, W.; Kammel, T.; Toubartz, M.; Steenken, S. *J. Am. Chem. Soc.* **1997**, *119*, 10673.
(8) a) Schmittel, M.; Keller, M.; Burghart, A. *J. Chem. Soc., Perkin Trans 2* **1995**, 2327. (b) Bockman, T. M.; Kochi, J. K. *J. Chem. Soc. Perlin Trans. 2* **1996**, 1633. (c) Schmittel, M.; Burghart, A.; Werner, H.; Laubender, M.; Söllner, R. *J. Org. Chem.* **1999**, 64, 3077.
(9) Kohno, Y.; Narasaka, K. *Bull. Chem. Soc. Jpn.* **1995**, *68*, 322.
(10) Sartori, G.; Maggi, R.; Bigi, F.; Arienti, G.; Casnati, G.; Bocelli, G.; Mori, G. *Tetrahedron* **1992**, *48*, 9483.
(11) Schmittel, M.; Steffen, J.-P.; Burghart, A. *Chem. Commun.* **1996,** 2349; Schmittel, M.; Steffen, J.-P.; Burghart, A. *Acta Chem. Scand.* **1999**, *53*, 781.
(12) (a) Schmittel, M.; Söllner, R. *Angew. Chem., Int. Ed. Engl.* **1996**, *35*, 2107. (b) Schmittel, M.; Söllner, R. *Chem. Ber./Recueil* **1997**, *130*, 771.
(13) Schmittel, M.; Söllner, R. *Chem. Commun.* **1998**, 565. Schmittel, M.; Söllner, R. *J. Chem. Soc., Perkin Trans. 2* **1999**, 515.
(14) Ogibin, Y. N.; Terent'ev, A. O.; Ilovaisky, A. I.; Nikishin, G. I. *Mendeleev Commun.* **1998**, 239. Fry, A. J.; Little, R. D.; Leonetti, J. *J. Org. Chem.* **1994**, *59*, 5017. Peek, R.; Streukens, M.; Thomas, H. G.; Vanderfuhr, A.; Wellen, U. *Chem. Ber.* **1994**, *127*, 1257.
(15) Grossert, J. S.; Yhard, G. B.; Pincock, J. A.; Curtis, J. M. *J. Mass Spectrosc.* **1996**, *31*, 761. Suh D.; Burgers, P. C., Terlouw, J. K. *Rapid Commun. Mass Spectrosc.* **1995**, *9*, 862.
(16) The expression *mesolytic* has been coined by Maslak and will be used throughout this paper: Maslak, P.; Narvaez, J. N. *Angew. Chem., Int. Ed. Engl.* **1990**, *29*, 283.
(17) Schmittel, M.; Trenkle, H. *J. Chem. Soc., Perkin Trans 2* **1996**, 2401.
(18) Some preliminary results have been published: Schmittel, M.; Trenkle, H. *Chem. Lett.* **1997**, 299.
(19) (a) Schmittel, M.; Röck, M. *Chem. Ber.* **1992**, *125*, 1611. (b) Schmittel, M.; Keller, M.; Burghart, A.; Rappoport, Z.; Langels, A. *Perkin Trans. 2* **1998**, 869.
(20) Nadler, E. B.; Rappoport, Z. *J. Am. Chem. Soc.* **1987**, *109*, 2122.
(21) Peters, K.; Peters, E.-M.; Schmittel M.; Trenkle H. *Z. Kristallogr.* **1998**, *213*, 105.
(22) Peters, K.; Peters, E.-M.; Schmittel, M.; Trenkle, H. *Z. Kristallogr.* **1997**, *212*, 467.
(23) Kaftory, M.; Nugiel, D. A.; Biali, S. E.; Rappoport, Z. *J. Am. Chem. Soc.* **1989**, *111*, 8181.
(24) All potentials are referred to the ferrocene/ferrocenium (Fc) couple unless otherwise noted. To obtain values vs SCE, simply add +0.39 V.

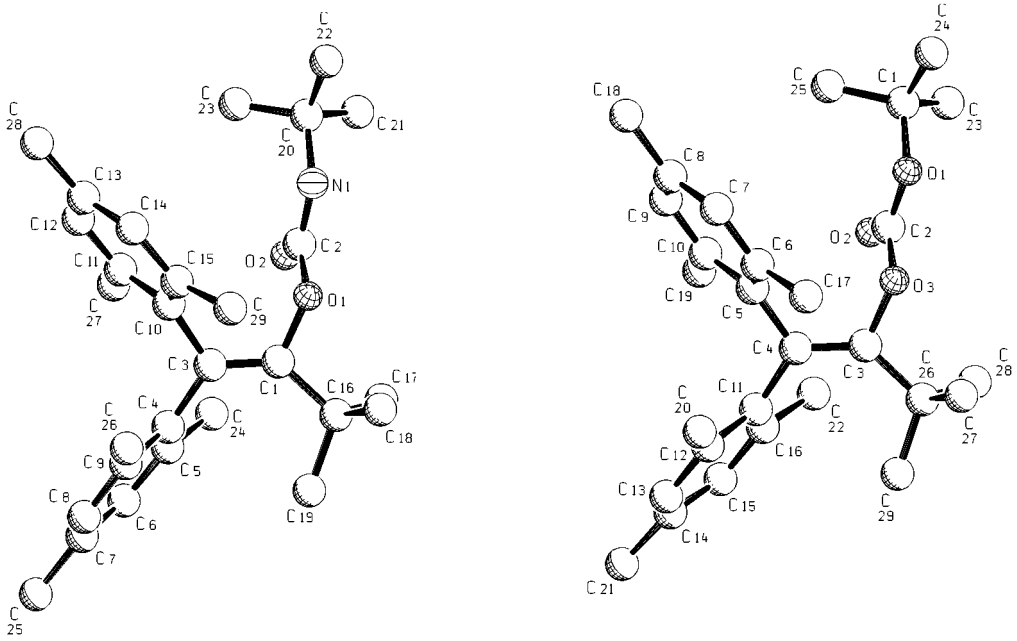

Figure 1. X-ray structure of **1a** (left) and **1b** (right).

Table 2. Selected Bond Lengths, Bond Angles, and Dihedral Angles of Some Model Compounds

	1a	1b	1g[a]	1h[b]
O−CO (Å)	1.376	1.364	1.345	1.296
C=C (Å)	1.323	1.343	1.329	1.331
C=C−O (Å)	1.421	1.428	1.451	1.443
∠C−O−C (deg)	116.8	116.6	117.3	119.9
∠C=C−O (deg)	116.5	116.1	116.4	115.6
∠O−C=O (deg)	123.4	125.8	124.0	129.9
∠C=C−O−C[c] (deg)	70.6	69.5	77.8	76.3
∠Mes_{cis}−C=C[d] (deg)	62.3	59.5	63.7	63.0
∠Mes_{trans}−C=C[e] (deg)	65.0	63.5	60.5	63.0

[a] Taken from ref 21. [b] Taken from ref 22. [c] Dihedral angle between the O−CO bond and the enol system. [d] Dihedral angle of the enol system and the *cis*-mesityl moiety. [e] Dihedral angle of the enol system and the *trans*-mesityl moiety.

Scheme 1. Products of the One-Electron Oxidation (Mesityl = 2,4,6-Trimethylphenyl)

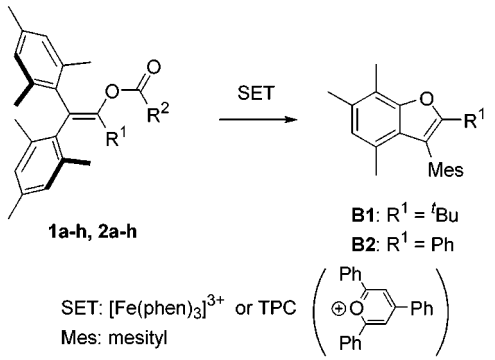

to **B1** was not detected and the unreacted starting material was recovered. Aside from **B1,2** no other products, e.g., derived from a nucleophilic attack in the β-position of the enol fragment or from direct cyclization reactions of the radical cation, as demonstrated earlier for the corresponding enol trifluoroacetate with R^1 = Ph (**2h**),[17] could be detected. The addition of tetrabromomethane or bromotrichloromethane as radical trapping agents had no sizable effect on the yields. The bisenol carbonate **3a** also provided benzofuran **B1** upon anodic oxidation (62% based on converted **3a** and considering two enol units in the oxidative transformation), while in the reaction with $[Fe(phen)_3]^{3+}$ or $Tl(CF_3COO)_3$, only the unreacted substrate was recovered. The low solubility of **1c** and **3b** prevented preparative one-electron oxidation studies.

Table 3. Preparative One-Electron Oxidation

	oxidant	oxidant (equiv)	benzofuran[a]	mass balance[b]
1a	$[Fe(phen)_3]^{3+}$	0.46	53	84
1a	$[Fe(phen)_3]^{3+}$	0.92	55	69
2a	$[Fe(phen)_3]^{3+}$	0.44	45	92
2a	$[Fe(phen)_3]^{3+}$	0.90	41	86
1b	$[Fe(phen)_3]^{3+}$	0.39	43	71
1b	$[Fe(phen)_3]^{3+}$	0.73	47	73
1b	TPC	0.51	42	69
1b	TPC	1.10	33	66
2b	$[Fe(phen)_3]^{3+}$	0.43	44	80
2b	$[Fe(phen)_3]^{3+}$	0.87	47	98
1d	$[Fe(phen)_3]^{3+}$	0.48	57	75
1d	$[Fe(phen)_3]^{3+}$	0.97	55	95
1e	$[Fe(phen)_3]^{3+}$	0.50		82
1e	$[Fe(phen)_3]^{3+}$	1.00	22	73
1e	$[Fe(phen)_3]^{3+}$	1.96	38	77

[a] Based on oxidation equivalents. [b] Based on starting enol ester.

Cyclic Voltammetry. The oxidation potentials of the carbamates and carbonates have been determined by cyclic voltammetry, providing irreversible oxidation waves at normal scan rates (20−500 mV s^{-1}), but reversible waves for all monoenol systems at high scan rates (≤5000 V s^{-1}) in acetonitrile or dichloromethane, allowing for the first time to determine the thermodynamic half-wave potentials of enol carbamates and carbonates (Table 4). The electron-rich enol esters **1e** and **1f** exhibit partially reversible oxidation waves even at low scan rates (>20 mV s^{-1}). Their oxidation potentials are much lower than for systems as **1d** or **1g**. All oxidation potentials are within an interesting range where chemical one-electron oxidation, photoinduced electron transfer as well as

(25) (a) Röck, M.; Schmittel, M. *J. Prakt. Chem.* **1994**, *336*, 325. (b) Schmittel, M.; Baumann, U. *Angew. Chem., Int. Ed. Engl.* **1990**, *29*, 541.

Table 4. Half-Wave Potentials[a] of Dimesitylenol Derivatives

system	E_{pa}[a] (V_{Fc})	$E_{1/2}$[b] (V_{Fc})	ΔE_p (mV)	system	E_{pa}[a] (V_{Fc})	$E_{1/2}$[b] ($V_{Fc}V$)	ΔE_p (mV)
1a	1.02	1.00	125	**2a**	0.99	0.99	170
1b	1.21	1.21	125	**2b**	1.06	1.06	190
1c	1.32	1.31	175				
1d	1.13	1.21	125				
1e		0.67[c]	68				
1f		0.35[c]	62				
1g	1.16[d]	1.16[d]	100	**2g**	1.04[d]	1.08[d]	155
1h	1.51[e]		85	**2h**	1.26[e]		190
3a	1.24						
3b	1.31						

[a] Measured at 100 mV s^{-1} in CH_3CN/0.1 M Bu_4NPF_6 and referenced to the ferrocene/ferrocenium couple; accuracy ±0.01 V. [b] In dichloromethane at scan rates $v = 500-5000$ V s^{-1}; accuracy ±0.02 V. [c] $E_{1/2}$ (100 mV s^{-1} in CH_3CN/0.1 M Bu_4NPF_6); accuracy ± 0.01 V. [d] Taken from ref 6. [e] Taken from ref 17.

anodic oxidation can be realized in the presence of many other functional groups.

The oxidation potentials provide a clear trend dependent on the electron-withdrawing nature of R^2 in the enol derivative $Mes_2C{=}C(R^1)OC(O)R^2$. Interestingly, in series **2a**−**h** (R^1 = Ph) the influence of R^2 on the oxidation potentials is much lower than in series **1a**−**d** and **1g**,**h** ($R^1 = Bu^t$). While in series **1a**−**d** and **1g**,**h** the electrophore is depicted by the enolate $Mes_2C{=}C{-}OC(O)R^2$, apparently there is a gradual change in **2a**−**h** from the $Mes_2C{=}C{-}OC(O)R^2$ to the $Mes_2C{=}C{-}Ph$ electrophore with increasing electron-withdrawing influence of R^2. Accordingly, in the electron-rich enol carbamate **2a** the electrophore is best represented by the $Mes_2C{=}C{-}O$ moiety, whereas in trifluoroacetate **2h** it rather resides on the $Mes_2C{=}C{-}Ph$ substructure. A different situation is met in **1e**,**f** since groups R^2 (*p*-$C_6H_4NMe_2$, ferrocenyl) are the best donor sites.

In more detailed cyclic voltammetric investigations, enol carbamate **1a** as well as carbonates **1b**, **2b**, and **1c**, *p*-methoxybenzoate **1d** as well as both bisenol derivatives showed intriguing curve crossings in the reverse scan at slow scan rates (20−50 mV s^{-1}) caused by the oxidation of electroactive follow-up products which are formed in a homogeneous reaction on the time scale of the experiment. In multisweep experiments, the complete reversible oxidation waves of these products could be observed allowing for the determination of their half-wave potentials. The potentials of the follow-up products of **1a**−**c**, **3a**−**b** and respectively those of **2a** and **2b**, were identical to the independently measured oxidation potentials of benzofurans **B1**[19a] ($E_{1/2}$ = 0.93 V_{Fc}[24]) and **B2**[25a] ($E_{1/2}$ = 0.87 V_{Fc}[24]), respectively. Digital simulation of the multisweep cyclic voltammograms of **1a**, based on a EC-CEC_{DISP} mechanism,[26,27] showed reasonable agreement with the experimental trace when using the same parameter set for benzofuran formation as described earlier (Figure 2).[6] Only the oxidation potentials and the first-order rate constant of the bond cleavage had to be adapted to the enol carbamate radical cation.

The enol esters **1e** and **1f** showed different behavior in cv experiments. Already at normal scan rates (100 mV s^{-1}) a partially reversible oxidation wave emerged at low potential due to the dimethylaniline ($E_{1/2}$(**1e**) = +0.67 V_{Fc}[24]) and the ferrocene donor ($E_{1/2}$(**1f**) = +0.35 V_{Fc}[24]). This assignment was tested for **1e** using ethyl *p*-dimethylaminobenzoate ($E_{1/2}$ = +0.64 V_{Fc}[24]) as a reference.

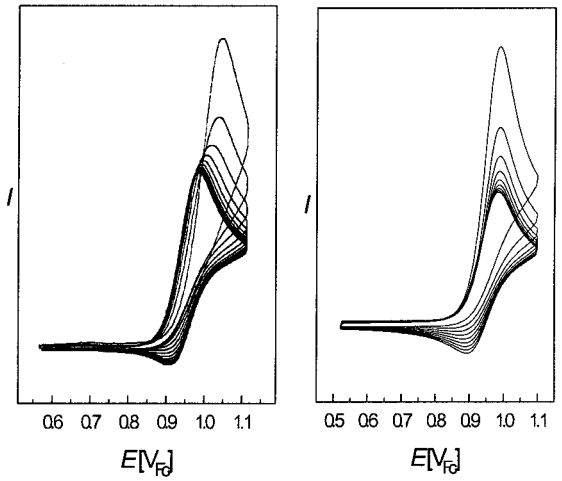

Figure 2. Multisweep cyclic voltammogram of **1a** in acetonitrile: left, experiment; right, digital simulation (details see Supporting Information).

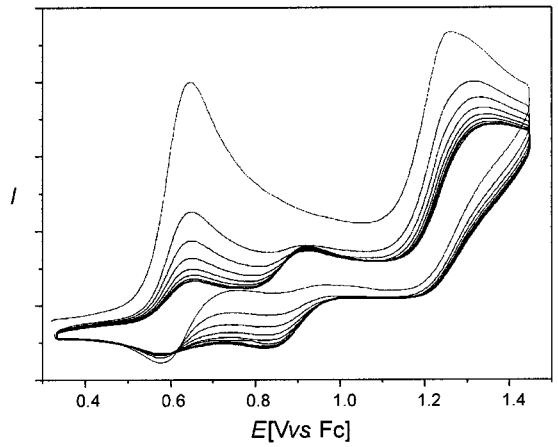

Figure 3. Multisweep-cv of **1e** at 500 mV s^{-1} in acetonitrile.

With both substrates a second irreversible wave (**1e**: E_{pa} = 1.32 V_{Fc},[24] **1f**: E_{pa} = 1.70 V_{Fc}[24]) showed up at higher potential. While oxidation of **1e** at v = 20 mV s^{-1} yielded an irreversible first oxidation wave at E_{pa} = 1.32 V_{Fc},[24] a completely reversible wave was afforded at $v \geq 2$ V s^{-1}. At these scan rates the ratio I_{pa} (at 1.32 V)/I_{pa} (at 0.67 V) reached a limiting value of 1.0. At v = 500 mV s^{-1} a reduction wave emerged, which in a multisweep experiment translated into a reversible wave assigned to benzofuran **B1** (Figure 3). In cv measurements of **1f** no formation of **B1** was registered, independent of whether the switching point was set after the first or second oxidation wave.

Enol carbonate **2b** showed already a partially reversible oxidation wave at scan rates >100 mV s^{-1} in dichloromethane. After the first oxidation wave, a second, irreversible wave occurred whose intensity increased at faster scan rates in the same manner as the reversibility of the first wave increased (Figure 4). As the reversibility of the first oxidation wave was decreased with increasing substrate concentration, this behavior is indicative of a second-order process limiting the rate of the follow-up

(26) "E" stands for electrochemical, "C" for chemical reaction step. For this type of reactions, the expression "DISP" has been established although this is no disproportionation reaction but an homogeneous electron-transfer equilibrium between the employed redox-active species.

(27) Heinze J. *Angew. Chem., Int. Ed. Engl.* **1984**, *23*, 831.

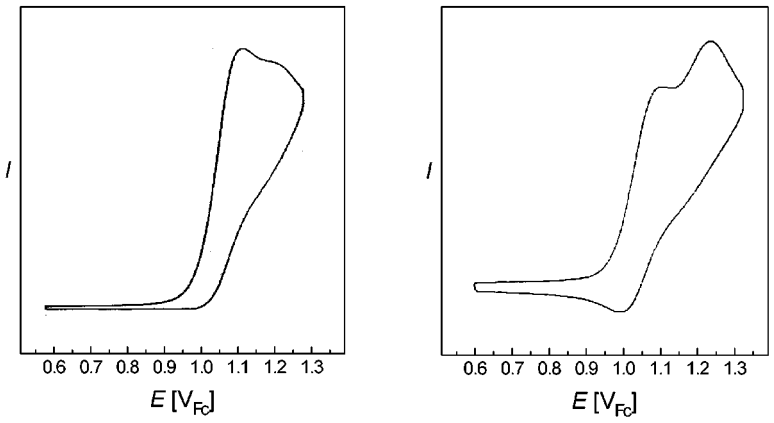

Figure 4. Cv of **2b** in dichloromethane: left, 50 mV s^{-1}; right, 500 mV s^{-1}.

Table 5. Rate Constants for the Mesolytic Cleavage of Enol Ester Radical Cations as Measured by Fast Scan Cyclic Voltammetry at Room Temperature

	$\mathbf{1a}^{\bullet+}$	$\mathbf{2a}^{\bullet+}$	$\mathbf{1b}^{\bullet+}$	$\mathbf{2b}^{\bullet+}$	$\mathbf{1d}^{\bullet+}$	$\mathbf{1e}^{\bullet+}$	$\mathbf{1g}^{\bullet+}$ [a]	$\mathbf{2g}^{\bullet+}$	$\mathbf{1h}^{\bullet+}$ [b]
k (CH_2Cl_2) (s^{-1})	502 ± 9	228 ± 2	104 ± 2	<2[c]	ca. 200	1.2 ± 0.01	110 ± 0.5[a]	ca. 50	
k (CH_3CN))s^{-1})	2870 ± 20	1650 ± 13	2020 ± 12	<1500[c]	ca. 5000	0.4 ± 0.01	ca. 5000		1.4 ± 0.02

[a] Taken from ref 6. [b] Taken from ref 17. [c] The exact rate constant could not be determined because the disproportionation reaction 2 $\mathbf{2b}^{+\bullet} \rightarrow \mathbf{2b}^{2+} + \mathbf{2b}$ becomes the rate-determining step as shown by concentration dependent cv experiments.

reaction of $\mathbf{2b}^{\bullet+}$. As a consequence, we assign the second wave to the oxidation of the persistent radical cation to the corresponding dication $\mathbf{2b}^{\bullet+} \rightarrow \mathbf{2b}^{2+}$ (E_{pa} = 1.13 V_{Fc},[24] 500 mV s^{-1}, CH_2Cl_2). Because of the small difference between the first and the second oxidation potential, the rate constant given in Table 5 can only provide an upper limit for the O−CO bond scission, as the disproportionation reaction of $\mathbf{2b}^{\bullet+}$ competes with the bond cleavage and restricts the lifetime of the radical cation.

In single sweep experiments, the bisenol carbonate **3a** exhibited the same qualitative cv behavior as **2b**. However, the slope of the cyclic voltammograms was rather small, presumably caused by a slow heterogeneous electron transfer which even prevented the occurrence of a pronounced reduction wave. In the cathodic back sweep, a slight crossing effect showed up and a reduction wave appeared at E_{pc} = 0.90 V_{Fc}[24] whose intensity depended on the scan rate and which could be assigned to the reduction of the benzofuran radical cation **B1**. In multisweep-experiments, the completely reversible oxidation wave of the follow-up product **B1**[19a] ($E_{1/2}$ = 0.93 V_{Fc}[24]) emerged (Figure 5), and the cv exhibited four isopotential points indicative of a clean conversion of **3a** into **B1**. In the case of bisenol oxalate **3b**, the waves for the first and the second oxidation step were not separated, attesting that the two enol electrophores are electronically insulated and the oxidation of one electrophore system has a rather small Coulombic influence on the second oxidation potential. The low solubility of **3b** prevented further investigations.

Fast Scan Cyclic Voltammetry. The kinetics of the mesolytic cleavage of the radical cations have been determined by fast scan cyclic voltammetry in acetonitrile and dichloromethane (Figure 6). When the scan rates were increased from 100 to 5000 V s^{-1}, the irreversible oxidation waves of all monoenol compounds turned reversible.[28] In the intermediate range, partially reversible waves were obtained showing the characteristics of

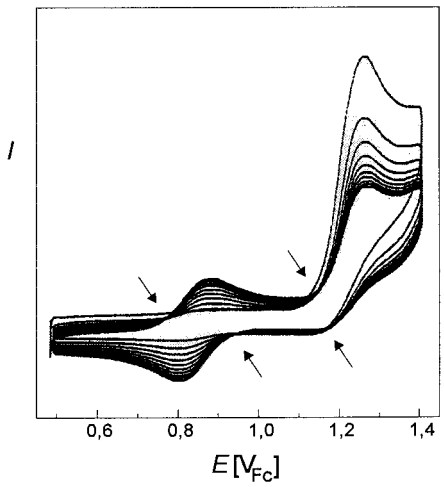

Figure 5. Multisweep-cv of **3a** in acetonitrile.

a typical EC-mechanism, i.e., a decreasing ratio $I_{pa}/v^{1/2}$ with increasing scan rate, an anodic shift of the peak potential with increasing v, and an increasing ratio I_{pc}/I_{pa} with increasing v that approached asymptotically the theoretical value 1 for a reversible one-electron oxidation. These data allow to determine the rate constants of the radical cation cleavage using the Nicholson-Shain formalism,[29] assuming a first-order process for systems **1a**, **2a**, **1b**, **2b**, **1d**, and **1e** (Table 5). Precise values for **1c** could not be obtained because of its low solubility and a strong electrode covering. Oxidation of **1f** did not reveal formation of **B1** so that a kinetic analysis was not meaningful.

Notably, the lifetime of the radical cations increased by a factor 5−50 when changing the solvent from dichloromethane to acetonitrile. To check for nucleophile-induced bond cleavage[30] the effect of methanol was probed; addition of less than 400 mol-% methanol to the acetonitrile solution had no significant effect on the

(28) Except for **1d**. In this case, only partially reversible oxidation waves could be obtained in acetonitrile.

(29) Nicholson, R. S.; Shain, I. *Anal. Chem.* **1964**, *36*, 6.

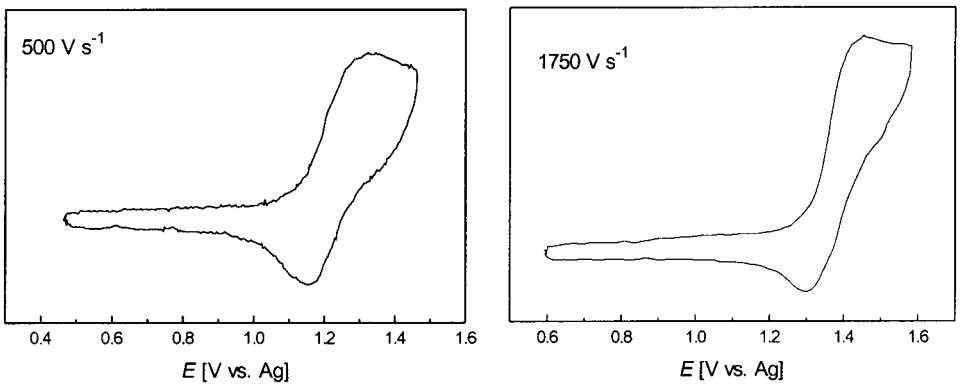

Figure 6. Fast scan cv of **1a** in dichloromethane (left) and acetonitrile (right).

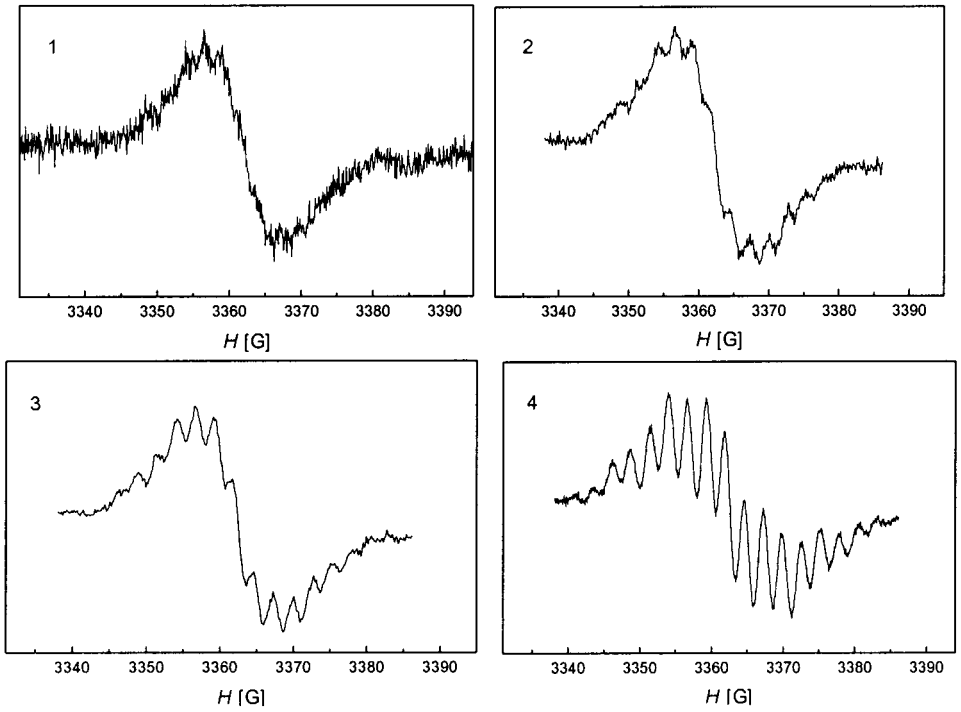

Figure 7. Change in the EPR spectrum after the oxidation of **2a** in the course of 4 h at 140 K (for details, see text).

lifetime of $\mathbf{1a}^{\bullet+}$. At higher concentrations of methanol the oxidation wave $\mathbf{1a}^{\bullet+} \rightarrow \mathbf{1a}^{2+}$ experienced a kinetic cathodic shift merging with the original wave $\mathbf{1a} \rightarrow \mathbf{1a}^{\bullet+}$. Hence, it is the dication that is trapped rapidly by methanol not the radical cation.

EPR of the Radical Cations and Fragmentation Products. At a high vacuum-line, the radical cations were generated by reaction of the enol derivatives with dioxygenyl hexafluoroarsenate[31] in chlorodifluoromethane at low temperature. In the oxidation of **2a** at 140 K a green solution resulted that afforded a signal without hyperfine splittings at $g = 2.0023$ (Figure 7). In the course of 4 h the spectrum converted slowly into a highly resolved signal with $g = 2.0026$, which could undoubtedly be assigned to the radical cation of the corresponding benzofuran **B2**.[32] The formation of benzofuran radical cations under conditions of the EPR experiment can be easily explained by the fact that the benzofuran possesses a lower oxidation potential than the model systems. Therefore, once the benzofuran is formed, it will be oxidized by the original $\mathbf{2a}^{\bullet+}$. Interestingly, when the dark green solution of $\mathbf{2a}^{\bullet+}$ was warmed to ca. 200 K for a few seconds a sudden change of color to dark violet occurred. The EPR spectrum of this solution measured again at 140 K showed a broad triplet with a coupling constant of $a^N = 22.9$ G and a g value of $g = 2.0017$ (Figure 8), which could be assigned to the *tert*-butylaminoacyl radical,[33] generated by mesolytic O−CO bond scission from $\mathbf{2a}^{\bullet+}$ (Scheme 2). The large coupling constant and the absence of an additional coupling to the N-H proton indicates that the radical adopts the *Z*-conformation from the parent enol carbamate **2a**. In line with former investigations on this radical,[33] no signs of interconver-

(30) Dinnocenzo, J. P.; Farid, S.; Goodman, J. L.; Gould, I. R.; Todd, W. P.; Mattes, S. L. *J. Am. Chem. Soc.* **1989**, *111*, 8973. Baciocchi, E.; Bernini, R.; Lanzalunga, O. *J. Chem. Soc., Chem. Commun.* **1993**, 1691. Todd, W. P.; Dinnocenzo, J. P.; Farid, S.; Goodman, J. L.; Gould, I. R. *Tetrahedron Lett.* **1993**, *34*, 2863. Herbertz, T.; Roth, H. D. *J. Am. Chem. Soc.* **1998**, *120*, 11904. Herbertz, T.; Roth, H. D. *J. Org. Chem.* **1999**, *64*, 3708.

(31) Dinnocenzo, J. P.; Banach, T. E. *J. Am. Chem. Soc.* **1986**, *108*, 6063.

(32) The EPR signals of the benzofuran radical cations including the hyperfine splittings are known from independent measurements. Schmittel, M.; Gescheidt, G.; Eberson, L.; Trenkle, H. *Perkin Trans.* 2 **1997**, 2145.

(33) Sutcliffe, R.; Ingold, K. U. *J. Am. Chem. Soc.* **1981**, *103*, 7686.

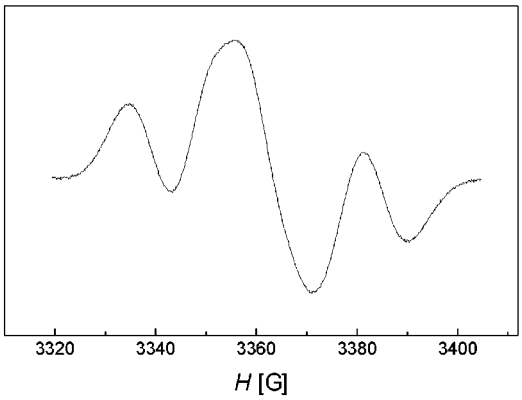

Figure 8. Detection of the butylaminoacyl radical ($a^N = 22.9$ G) from **2a**$^{+\bullet}$.

Scheme 2

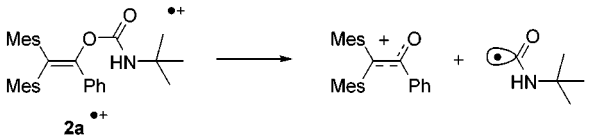

Table 6. EPR of Enol Carbamate and Enol Carbonate Radical Cations

	1a$^{+\bullet}$	**2a**$^{+\bullet}$	**1b**$^{+\bullet}$	**2b**$^{+\bullet}$
g value	2.0015	2.0023	2.0014	2.0023

sion to the *E*-isomer could be detected on the time scale of the EPR experiment. The triplet signal is superimposed by an additional singlet signal, derived from the radical cation **2a**$^{\bullet+}$ with $g = 2.0023$.

Enol carbonates **1b** and **2b** as well as enol carbamate **1a** provided also unresolved EPR spectra at 140 K in chlorodifluoromethane solution upon oxidation with O_2-AsF_6. The *g* values are given in Table 6.

Discussion

The Nature of the Enol Radical Cations. From the X-ray structure of **1a** and **1b** one can derive that the enol π system and the O−CO bond are almost orthogonal (70 ± 1° for **1a** and **1b)**, which should allow for convenient overlap of the scissile σ(O−CO) and the π(C=C) system. While these data do not reveal details about the corresponding odd-electron cations, some important information can be derived from the unresolved EPR spectra of the enol carbonate and carbamate radical cations. Although no statement about the spin density distribution is possible, the absence of couplings to the nitrogen in the enol carbamate radical cations indicates that the positive charge and the spin density are delocalized in the π-system of the enol moiety rather than in the σ(O−C) bond. As the *g* values depend only on the nature of the substituent in 1-position and show equal values for **1b**$^{\bullet+}$ and **1a**$^{\bullet+}$, respectively for **2b**$^{\bullet+}$ and **2a**$^{\bullet+}$, one can suppose that the nature of the SOMO is similar for most model systems (**a**−**d**). Decisively different is the situation with **1e**,**f**. The oxidation potentials indicate that for the latter systems the key electrophore is now the electron-rich acyl group.

Mesolytic O−CO Bond Cleavage. The formation of benzofurans **B1** and **B2**, respectively as one-electron oxidation products of the enol systems implicates that at some stage of the overall reaction O−CO bond cleavage must take place. As such the situation is reminiscent of the chemistry of enols and different enol derivatives C=C−O−X after one-electron oxidation with X = SiR_3, $TiCp_2Cl$, $P(OEt)_2$, and others.[11−13] With those substituents, the mesolytic bond cleavage at the stage of the enol radical cation could be established and the formation of the benzofurans traced down to the mechanism depicted in Scheme 3. In all bond cleavage processes, the group X was cleaved off as cationic fragment thus resulting in the formation of an α-carbonyl radical which was further oxidized under the reaction conditions. Cyclization of the α-carbonyl cation, [1,2]-methyl shift and deprotonation finally lead to the benzofuran. This mechanistic scheme could additionally be confirmed by preparative and cyclic voltammetry studies indicating that benzofuran formation can equally be triggered by oxidation of enolates.

Scheme 3. Formation of Benzofuran by O−X Bond Dissociation of the Enol Radical Cation[11−13]

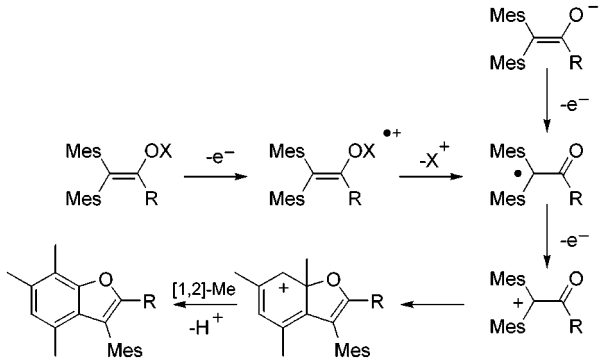

Scheme 4

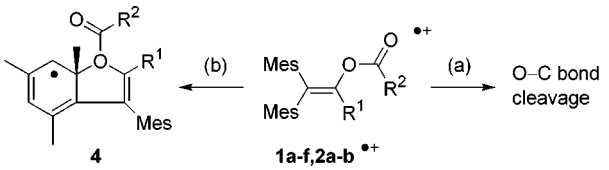

For the various enol ester radical cations of this study two distinct reaction pathways to the benzofurans need to be considered: (a) O−C bond dissociation of the enol ester radical cations in analogy to the examples above or (b) cyclization on the stage of the radical cation followed by O−C bond cleavage at a later stage of the reaction (Scheme 4). Dissociative electron transfer, a process well-known for radical anion bond cleavage reactions,[34] can easily be discarded since the radical cations could be observed both by cyclic voltammetry and EPR spectroscopy.

Three arguments strongly favor mechanism (a) over (b): (1) the steric crowding in the transition state and in the distonic radical cation along route (b) is prohibitive[35] according to AM1[36] (when $R^1 = Bu^t$ and $R^2 = OMe$), and (2) one would expect that the formed distonic radical cation should easily be oxidized at the radical site. The oxidation potential of the cyclohexadienyl radical has

(34) Savéant, J.-M. *Acc. Chem. Res.* **1993**, *26*, 455. Donkers, R. L.; Maran, F.; Wayner, D. D. M.; Workentin, M. S. *J. Am. Chem. Soc.* **1999**, *121*, 7239.

(35) According to our AM1 calculations, **4** is not local minimum structure but readily opens to **1**$^{\bullet+}$.

(36) Dewar, M. J. S.; Zoebisch, E. G.; Healy, E. F.; Stewart, J. J. P. *J. Am. Chem. Soc.* **1985**, *107*, 3902.

Scheme 5. Mechanistic Alternatives for the O−C Bond Cleavage

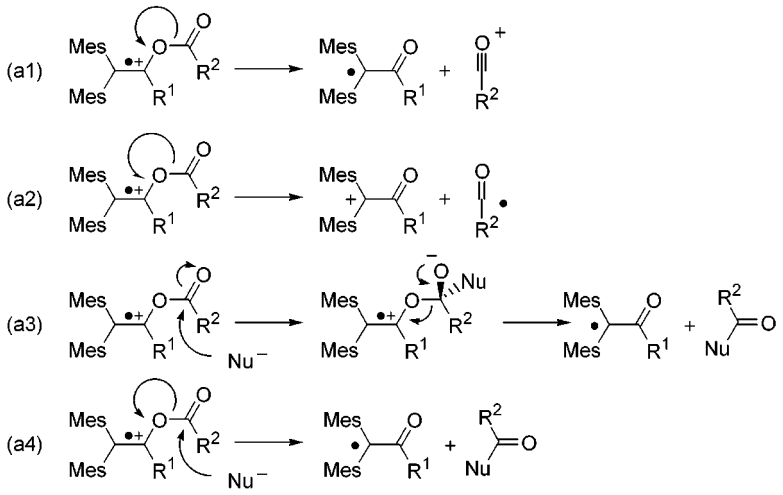

Table 7. Ionization and Solution Oxidation Potentials of Various Radicals

	5•	6•	^{t}BuNHCO•	^{t}BuOCO•	*p*AnCO•	CH_3CO•	CF_3CO•
IP_a[a]/eV	6.87	6.87	7.45	8.22	7.01	7.72	9.16
$E_{1/2}/V_{Fc}$ (calcd)[b]	0.12	0.12	0.56	1.14	0.23	0.76	1.86
$E_{1/2}/V_{Fc}$ (calcd)[c]	−0.19	−0.19	0.41	1.21	−0.05	0.69	2.19
E_{pa}/V_{Fc} *d* (expt)	0.14	0.24					

[a] Adiabatic ionization potential calculated by AM1. [b] Solution oxidation potential calculated using Gassman's[40] correlation. [c] Solution oxidation potential calculated using Wayner's correlation.[41] [d] Irreversible anodic peak potentials.

been determined by Wayner and Griller[37] to be $E_{1/2}$ = −0.04 V vs SCE (−0.43 V_{Fc}[24]). Even when we consider a strong anodic shift in **4** because of the electron-withdrawing oxonium ion it is hard to conceive that **4** will exhibit an $E_{1/2}^{ox} \geq 1$ V_{Fc}.[24] Accordingly, **4** should be more easily oxidized than the parent enol ester. The cyclic voltammmetry experiments, however, indicate clearly that the irreversible wave in the enol ester oxidation represents only the transfer of one, but not of two electrons, thus eliminating pathway (b) as a plausible mechanistic alternative. (3) In the dissociation of **1a**$^{\bullet+}$ we find the aminoacyl radical as product whose formation cannot be explained with **4** being an intermediate.

Selectivity of Bond Cleavage. For systems **a**−**d** the donor site is clearly the enol moiety. Hence, the mechanism of the O−C bond cleavage according to pathway (a) may now be classified along three distinct mechanistic alternatives: Either it involves (a1) a heterolytic, (a2) a homolytic, or (a3) a special type of nucleophile induced bond cleavage as represented in Scheme 5. While for the first two reaction modes there are well-characterized examples in the literature,[4,11−13,38] pathway (a3) would involve a two-step process that has not been established in the literature in contrast to one-step nucleophile-induced bond cleavage reactions.[30] A concerted mechanism (a4), however, does not make sense in light of the well-known addition elimination chemistry at carbonyl sites.

A bimolecular cleavage process along route (a3) can be rather convincingly ruled out on the basis of our kinetic data in comparison with systems for which a nucleophile-assisted bond-cleavage process has been established (vide infra). The outcome of a monomolecular bond cleavage either according to (a1) or (a2) should easily be predictable from a simple thermochemical cycle calculation since it ought to depend only on the redox potentials of the two radicals formed in the putative homolytic cleavage of the neutral compound. From cv investigations of the corresponding enolates, the oxidation potentials of the α-carbonyl radicals[39] are known to be $E_{1/2}$ (**5**•) = 0.14 V_{Fc}[24] and $E_{1/2}$ (**6**•) = 0.24 V_{Fc}.[24]

Unfortunately, the solution oxidation potentials of the acyl radicals with R^2 = Me, CF_3, OBu^t, and NHBu^t are not known. As a consequence, we have resorted to adiabatic ionization potentials IP_a calculated by the AM1 method[36] which obviously reflect the gas-phase situation. To extract solution data we have used well-established correlations of oxidation potentials in solution and ionization energies (i.e., those of Gassman:[40] $E_{1/2}$ [V_{Fc}] = 0.76 IP_a − 5.10 and of Wayner:[41] $E_{1/2}$ [V_{Fc}] = 1.043 IP_a − 7.36).

Using the experimental data from **5**• and **6**• as a reference (Table 7) it becomes evident that for our class of intermediates Gassman's correlation provides reasonable solution oxidation potentials in combination with AM1 calculations. As the oxidation potentials of all acyl radicals (except for pAnCO•) are decisively higher than that of **5**• and **6**• it is save to predict that the cleavage of enol ester radical cations **1a**−**c**,**2a**,**b**$^{\bullet+}$ will directly lead to α-carbonyl cations and acyl radicals. In former investigations, this cleavage selectivity could be confirmed

(37) Wayner, D. D. M.; McPhee, D. J.; Griller, D. *J. Am. Chem. Soc.* **1988**, *110*, 132.
(38) Mariano, P. S. *Acc. Chem. Res.* **1983**, *16*, 130; Lan, A. J. Y.; Quillen, S. L.; Heuckeroth, R. O.; Mariano, P. S. *J. Am. Chem. Soc.* **1984**, *106*, 6439. Yoshiyama, T.; Fuchigami, T. *Chem. Lett.* **1992**, 1995. Akaba, R.; Niimura, Y.; Fukushima, T.; Kawai, Y.; Tajima, T.; Kuragami, T.; Negishi, A.; Kamata, M.; Sakuragi, H.; Tokumaru, K. *J. Am. Chem. Soc.* **1992**, *114*, 4460. Zhang, X.; Yeh, S.-R.; Hong, S.; Freccero, M.; Albini, A.; Falvey, D. E.; Mariano, P. S. *J. Am. Chem. Soc.* **1994**, *116*, 4211. Fuchigami, T.; Fujita, T. *J. Org. Chem.* **1994**, *59*, 7190. Mizuno, K.; Tamai, T.; Hashida, I.; Otsuji, Y. *J. Org. Chem.* **1995**, *60*, 2935. Fukuzumi, S.; Yasui, K.; Itoh, S. *Chem. Lett.* **1997**, 161. Baciocchi, E.; Crescenzi, C.; Lanzalunga, O. *Tetrahedron* **1997**, *53*, 4469. Su, Z.; Mariano, P. S.; Falvey, D. E.; Yoon, U. C.; Oh, S. W. *J. Am. Chem. Soc.* **1998**, *120*, 10676.
(39) Röck, M.; Schmittel, M. *Chem. Commun.* **1993**, 1739.
(40) Gassman, P. G.; Yamaguchi, R. *J. Am. Chem. Soc.* **1979**, *101*, 1308.
(41) Wayner, D. D. M.; Sim, B. A.; Dannenberg, J. J. *J. Org Chem.* **1991**, *56*, 4853.

experimentally for the enol acetate $\mathbf{1g}^{\bullet+}$.[6] The detection of the *tert*-butylaminoacyl radical in the EPR experiments of $\mathbf{1a}^{\bullet+}$ shows that the oxidative cleavage of the enol carbamates follows the same selectivity. Therefore, on the basis of the semiempirical calculations one can conclude that model systems $\mathbf{1a}-\mathbf{d},\mathbf{2a},\mathbf{b}^{\bullet+}$ undergo a homolytic bond scission according to (a2).

Mesolytic Bond Cleavage of Special Systems. A different situation is met in the oxidative decomposition of **1e**. The preparative oxidation and the cv data, in particular the concentration independence of the kinetics, indicate that $\mathbf{1e}^{\bullet+}$ undergoes slow O−CO bond cleavage. Thermodynamic arguments propose that monomolecular fragmentation should result in formation of the aminobenzoyl cation (IP_a = 6.47 eV, $E_{1/2}$ (calcd) = −0.18 V_{Fc}) and the α-carbonyl radical. Since the charge in $\mathbf{1e}^{\bullet+}$ is originally located on the aminobenzoyl group, this cleavage occurs in the homolytic fashion. The positive charge on the aminobenzoyl residue both in $\mathbf{1e}^{\bullet+}$ and after cleavage in the acyl cation nurtured our hope that $\mathbf{1e}^{\bullet+}$ might undergo O−CO bond cleavage in the presence of a nucleophile via pathway a3 (see Scheme 5). However, no change in reversibility was registered upon addition of up to 10 equivalents of methanol. In contrast, a drastic change was detected in the cv with pyridine, but this is due to deprotonation at the methyl groups as demonstrated by control experiments with ethyl *p*-dimethylaminobenzoate. With good nucleophiles that are less basic, i.e., trimethylsilyl azide, as nucleophiles again reversibility over the a scan range 50−500 mV s^{-1} is the same as in pure acetonitrile.

No cleavage occurred after oxidation of **1f**. The corresponding radical cation is apparently a persistent ferrocinium type species. Intramolecular activation of the scission with ferrocene as redox relay is not operative.

While oxidative cleavage of **3a** is observed in the cv experiments and in anodic oxidation (furnishing two equivalents of benzofuran), the failure to oxidatively cleave **3a** using one-electron oxidants indicates that the bond scission is very slow and cannot compete with back electron transfer to the original oxidant. Presumably, bond cleavage is sluggish because of stereoelectronic reasons, as the dihedral angle between σ(O−CO) and π-(C=C)O assumes Φ = 50°.

Kinetics and Thermodynamics of the Mesolytic O−CO Bond Cleavage. Table 5 shows the rate constants for the mesolytic cleavage of the O−CO bond in various enol ester type radical cations. Most of them fall in a narrow range, except those of enol carbonate **2b**, enol ester **1e**, and trifluoroacetate **1h**. The small variation in the rate constants of enol acetates, carbonates, and carbamates once again confirms the homolytic cleavage mode, as one would expect greater variations in k_f for the heterolytic mode because of the vastly different oxidation potentials of the acyl radicals. Furthermore, the bimolecular cleavage process, e.g., a new nucleophile-assisted bond cleavage (a3), can also be ruled out by the kinetic data, as the activation entropy of the mesolytic cleavage of $\mathbf{1g}^{\bullet+}$ is positive[6] (+11 cal mol^{-1} K^{-1}) in line with a dissociative process in the rate-determining step.

What is the reason for the slow oxidative bond dissociation of **2b**, **1e**, and **1h**? For **1e** the situation is clear, as the low oxidation potential (Table 4) decreases the thermochemical driving force ΔG_{Meso} for the bond cleavage according to Scheme 6. Hence, when the data in Table 5 are analyzed the deceleration of the mesolytic bond cleavage in the case of $\mathbf{2b}^{\bullet+}$ and $\mathbf{1h}^{\bullet+}$ is most surprising.

Scheme 6. Thermochemical Cycle for the Evaluation of ΔG_{Meso} (CR = α-carbonyl Radical)

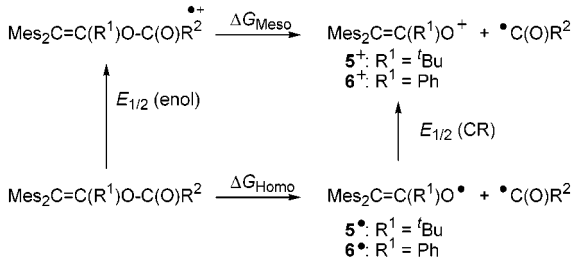

For **2b**, an additional important observation stems from a comparison of the mesolytic cleavage of **1a**,**b**,**2a**,$\mathbf{b}^{\bullet+}$. While for enol carbamates ($k_f(\mathbf{1a}^{\bullet+})/k_f(\mathbf{2a}^{\bullet+})$ = 2.2) the ratio of the rates is very small, it is markedly increased for the analogous enol carbonates ($k_f(\mathbf{1b}^{\bullet+})/k_f(\mathbf{2b}^{\bullet+})$ = 52).[42] To understand this difference, we have analyzed the thermodynamics of the mesolytic bond cleavage (Scheme 6) in detail.

According to thermochemical cycle calculations,[43] the mesolytic bond energy ΔG_{Meso} can be derived from the homolytic bond energy and the oxidation potentials of reactant and the α-carbonyl radical (CR): $\Delta G_{Meso} = \Delta G_{Homo} - nF[E_{1/2}(\text{enol}) - E_{1/2}(\text{CR})]$.

Because of the cross-conjugation of the phenyl group, ΔG_{Homo} in both the carbamates and the carbonates is expected to be roughly 8 kJ mol^{-1} lower for series **2** (R^1 = Ph) molecules as compared to those of series **1** (R^1 = Bu^t).[44] However, this difference in homolytic bond energies $\Delta\Delta G_{Homo} = \Delta G_{Homo}(\mathbf{2}) - \Delta G_{Homo}(\mathbf{1})$ is basically compensated by the difference in the oxidation potentials of the α-carbonyl radicals $\Delta E_{1/2}(\text{CR}) = E_{1/2}(\mathbf{6}^{\bullet}) - E_{1/2}(\mathbf{5}^{\bullet})$ = 0.09 V (8 kJ mol^{-1}).[45] As a consequence, the differences in mesolytic bond cleavage energies $\Delta\Delta G_{Meso} = \Delta G_{Meso}(\mathbf{2}) - \Delta G_{Meso}(\mathbf{1})$ are determined only by $nF[E_{1/2}(\mathbf{2}) - E_{1/2}(\mathbf{1})]$. The small difference in the oxidation potentials of the enol carbamates leads to similar values of ΔG_{Meso} for $\mathbf{1a}^{\bullet+}$ and $\mathbf{2a}^{\bullet+}$, whereas ΔG_{Meso} is increased in enol carbonate $\mathbf{2b}^{\bullet+}$ with respect to $\mathbf{1b}^{\bullet+}$ by 14.5 kJ mol^{-1} because of $\Delta E_{1/2}$ = 0.15 V. Hence, the rate difference can readily be explained by the thermodynamics of the mesolytic bond cleavage.

A different effect is responsible for the drastic change of rate between $\mathbf{1h}^{\bullet+}$ and $\mathbf{1g}^{\bullet+}$, but that has been discussed previously.[17]

Bond Cleavage at the Dication Stage. For **2b**, a third mechanistic possibility has to be discussed since the rate-determining step proved to be dependent on the concentration of **2b**. Both at higher scan rates and at lower concentration the first oxidation wave turns reversible and an irreversible wave shows up at more anodic potential. According to the cv of **2b** in dichloromethane (Figure 4), the potential difference between the first and the second oxidation is as small as 140 mV. Because mesolytic cleavage in dichloromethane is slow,

(42) The same trend is seen in acetonitrile, but it is not possible to quantify the effect since the observed rate constants represent only an upper limit for the mesolytic cleavage because of disproportionation reactions.

(43) Wayner, D. D. M.; Parker, V. D. *Acc. Chem. Res.* **1993**, *26*, 287.
(44) Based on the AM1 calculated homolytic bond energies.
(45) Röck, M.; Schmittel, M. *Chem. Commun.* **1993**, 1739.

the main reaction pathway of $\mathbf{2b}^{\bullet+}$ is now disproportionation into neutral **2b** and $\mathbf{2b}^{2+}$. This interpretation is supported by the concentration dependence of the reduction wave of $\mathbf{2b}^{\bullet+}$, which decreases with increasing concentration.

For enol carbamate **2a**, a similar effect was observed in the presence of higher concentrations of methanol. The more methanol was added, the smaller was the potential difference between the first reversible wave of the carbamate and a second irreversible wave. This behavior can readily be rationalized if the second wave is assigned to the oxidation of $\mathbf{2a}^{\bullet+} \rightarrow \mathbf{2a}^{2+}$ as the addition of methanol increases the rate of the follow-up reaction of the dication by nucleophilic attack. This leads to a cathodic shift of the oxidation wave, which is typical for EC_{irr}-mechanisms.

Additional irreversible oxidation waves at higher anodic potentials are also registered for **1e** ($E_{pa} = 1.32$ V_{Fc}[24]) and **1f** ($E_{pa} = 1.70$ V_{Fc}). While the first oxidation occurs at the *p*-dimethylaniline and ferrocene site, respectively, the second oxidation is due to removal of an electron from the enol moiety. This assignment is supported by the oxidation potential of the protonated enolester $\mathbf{1e\text{-}H}^{+}$ ($E_{pa} = 1.28$ V_{Fc}), which should have an electronic structure similar to that of $\mathbf{1e}^{\bullet+}$.

Quantitative formation of **B1** is only detected in cv experiments, when the dication $\mathbf{1e}^{2+}$ is formed, which obviously cleaves to yield two cationic fragments. In contrast to the latter case, no **B1** is detected in preparative oxidations or cv measurements from either $\mathbf{1f}^{\bullet+}$ or $\mathbf{1f}^{2+}$. While the oxidation of the ferrocene moiety in $\mathbf{1f}^{\bullet+}$ is completely reversible even at low scan rates ($v = 20$ mV s^{-1}), the second oxidation is expected to result in bond cleavage as indicated by the irreversible cv wave. Due to the high potential, however, benzofuran **B1** is formed as an unstable dication at $E_{pa} > 1.70$ V_{Fc}[46] that decomposes and precludes the detection of the $\mathbf{B1}^{\bullet+} \rightarrow \mathbf{B1}$ redox process.

Conclusion

We have investigated the O−CO bond scission in different enol ester, carbamate and carbonate radical cations and probed various mechanistic possibilities. It could be shown by EPR experiments and thermochemical cycle considerations that the cleavage selectivity of the O−CO bond scission follows a monomolecular, homolytic pathway both for electron-rich and electron-poor derivatives. The rate constants of the mesolytic bond cleavage are for most investigated compounds in a very similar range (k (CH_3CN) = (2−5) × 10^3 s^{-1}). All attempts to find a nucleophile-induced pathway via a addition−elimination mechanism were met with failure.

Experimental Section

General Aspects. 250 MHz ^{1}H NMR and 150 MHz ^{13}C NMR spectra were recorded in $CDCl_3$ on a Bruker A250 or a Bruker DMX600. Chemical shifts are reported in ppm downfield vs the internal standard TMS. The abbreviation br. designates signals broadened by coalescence. IR spectra were recorded in KBr using a Perkin-Elmer FT-IR1605 infrared spectrometer. Mass spectra were recorded on a Finnigan MAT 8200 Mass spectrometer using electron ionization (EI) at 70 eV. Elemental analyses were performed at the institute of inorganic chemistry, University of Würzburg. Melting points were taken on a Büchi Smp-20 apparatus and are uncorrected. Theoretical studies were performed with the help of the AM1 molecular orbital method.[36] The geometries of the radical cations were optimized by using the unrestricted Hartree−Fock (UHF) formalism. Heats of formation were calculated from the UHF-optimized structures by utilizing the half-electron (HE) method. Adiabatic ionization potentials (IP_a) were obtained as the difference in the heat of formation between the species involved in the redox process.

Materials. Commercial reagents were purchased from standard chemical suppliers and were used without further purification. Acetonitrile for cv and one-electron oxidations was purchased in HPLC quality from Riedel-de-Haën, distilled over calcium hydride and filtered through basic alumina (ICN). The preparation of the corresponding enols has been reported elsewhere.[19a,25a]

2-(*tert*-Butylaminocarbonyloxy)-1,1-dimesityl-3,3-dimethyl-1-butene (1a). A suspension of 60% NaH in paraffin oil (1.80 g, 45.0 mmol) was washed under nitrogen atmosphere with 25 mL of dry *n*-pentane, suspended in 10 mL of dry THF, and then added to a solution of 1,1-dimesityl-3,3-dimethylbut-1-en-2-ol (1.01 g, 3.00 mmol) in dry THF (30 mL). The mixture was stirred for 20 min at room temperature and excess NaH was filtered off under nitrogen atmosphere. *tert*-Butylisocyanate (3.0 mL, 30.0 mmol) was added, and the mixture was allowed to stir for 24 h. After hydrolysis, the aqueous layer was extracted three times with ether. The combined organic layers were first washed with saturated $NaHCO_3$ and water and then dried over Na_2SO_4. Removal of the solvent, filtration over silica gel (using dichloromethane/cyclohexane 1:2), and recrystallization from ethanol afforded 0.50 g (1.15 mmol, 38%) of pure **1a** as a white solid: mp 140 °C; IR (KBr) = 3644, 3495, 3447, 3348, 1739, 1611 cm^{-1}; ^{1}H NMR δ 0.95 (s, 9 H), 1.02 (s, 9 H), 1.88 (br s, 6 H), 2.16 (s, 3 H), 2.20 (s, 3 H), 2.40 (br s, 3 H), 2.75 (br s, 3 H), 4.04 (s, 1 H), 6.60 (br s, 2 H), 6.80 (br s, 2 H); ^{13}C NMR δ 20.49, 20.94, 28.22, 28.38, 38.72, 49.59, 124.06, 127.57, 127.77, 128.73, 130.24, 134.95, 135.26, 135.39, 135.83, 137.5, 138.19, 138.95, 140.18, 152.79 (C2), 153.03. Anal. Calcd for $C_{29}H_{41}NO_2$: C, 79.95; H, 9.49; N, 3.22. Found: C, 79.67; H, 9.45; N, 3.13.

1,1-Dimesityl-2-*tert*-butyllithium Enolate. Under nitrogen atmosphere, 14 mL (21 mmol) of a 1.5 M solution of *t*-BuLi in pentane was added to 200 mL of an ethereal solution of dimesitylketene (7.82 g, 28.1 mmol) during 1 h at −40 °C. After being stirred for 3 h, the mixture was allowed to warm to room temperature.

1,1-Dimesityl-3,3-dimethyl-2-*tert*-butoxycarbonyloxy-1-butene (1b). To a solution of 1,1-dimesityl-2-*tert*-butyllithiumenolate (12.4 mmol) in 80 mL of dry ether was added di-*tert*-butyl carbonate (4.10 g, 18.6 mmol), and the mixture was stirred for 20 min. After addition of additional di-*tert*-butyl carbonate (2.70 g, 12.4 mmol), the mixture was stirred overnight and the white precipitate was filtered off. The filtrate was washed with 5% NaOH, water, saturated $NaHCO_3$, and again with water. After drying, it was concentrated to a red oil that was purified by column chromatography on silica gel (hexane/dichloromethane 1:1) to yield 1.33 g (3.05 mmol, 25%) of pure **1b** as white crystals: mp 127 °C; IR (KBr) 1748, 1610 cm^{-1}; ^{1}H NMR δ 1.03 (s, 9 H), 1.08 (s, 9 H), 1.87 (br s, 6 H), 2.15 (s, 3 H), 2.20 (s, 3 H), 2.40 (s, 3 H), 2.72 (br s, 3 H), 6.61 (d, 2 H), 6.82 (s, 2 H); ^{13}C NMR δ 20.58, 20.82, 27.19, 28.45, 38.70, 81.05, 124.26, 127.66, 128.23, 128.92, 129.96, 134.42, 134.75, 135.65, 136.07, 151.81, 152.68. Anal. Calcd for $C_{29}H_{40}O_3$: C, 79.77; H, 9.10 Found: C, 79.83; H, 9.23.

1,1-Dimesityl-3,3-dimethyl-2-benzyloxycarbonyloxy-1-butene (1c). To a solution of 1,1-dimesityl-2-*tert*-butyllithium enolate (12.4 mmol) in 80 mL of dry ether was added a solution of carbobenzoxychloride (4.00 g, 23.4 mmol) in 10 mL of dry ether, and the mixture was stirred for 20 min. After addition of another 2.70 g (15.6 mmol) of carbobenzoxy chloride, the mixture was stirred overnight and the white precipitate was filtered off. The filtrate was washed with 5% NaOH, water, saturated $NaHCO_3$, and water. After drying, it was concentrated to leave a red oil which was purified by column

(46) $\mathbf{B1}^{\bullet+} \rightarrow \mathbf{B1}^{2+}$: $E_{pa} = +1.66$ V_{Fc} (at 100 mV s^{-1} in acetonitrile). Schmittel, M.; Langels, A. *J. Org. Chem.*, **1998**, *63*, 7328.

chromatography on silica gel (hexane/dichloromethane 1:1) to yield 0.83 g (1.76 mmol, 11%) of **1c**: mp 160 °C; IR (KBr) 1749, 1608 cm^{-1}; ^1H NMR δ 1.07 (s, 9 H), 1.89 (br s, 6 H), 2.20 (s, 3 H), 2.22 (s, 3 H), 2.44 (s, 3 H), 2.73 (s, 3 H), 4.80 (s, 1 H), 4.90 (s, 1 H), 6.57 (s, 1 H), 6.64 (s, 1 H), 6.83 (s, 2 H), 6.95 (m, 2 H), 7.27 (m, 3 H); ^{13}C NMR δ 20.78, 28.42, 38.81, 69.15, 125.38, 127.57, 127.95, 128.27, 128.96, 129.94, 133.94, 134.38, 135.30, 135.85, 136.29, 152.81, 153.63. Anal. Calcd for $C_{32}H_{38}O_2$: C, 81.66; H, 8.14. Found: C, 81.36; H, 7.87.

1,1-Dimesityl-2-(*p*-methoxybenzoyloxy)-3,3-dimethyl-1-butene (1d). Reaction of 1,1-dimesityl-3,3-dimethylbuten-2-ol (1.80 g, 5.35 mmol) and sodium hydride (138 mg, 5.75 mmol) with 4-methoxybenzoyl chloride (1.00 g, 5.86 mmol) by the method described before yielded 1.59 g (3.38 mmol, 63%) of pure **1d** after chromatography (silica gel, toluene) as a white solid: mp 157 °C; IR (KBr) 1730, 1610 cm^{-1}; ^1H NMR δ 1.10 (s, 9 H), 1.94 (br s, 6 H), 2.03 (s, 3 H), 2.23 (s, 3 H), 2.54 (br s, 3 H), 2.85 (br s, 3 H), 3.82 (s, 3 H), 6.5−6.8 (br.m, 4 H), 6.84 (d, ^3J = 7.0 Hz, 2 H), 7.83 (d, ^3J = 7.0 Hz, 2 H); ^{13}C NMR δ 20.57, 20.81, 28.64, 39.28, 55.32,113.4, 122.61, 125.67, 128.65, 131.38, 134.92, 135.41, 136.08,138.05, 151.75, 163.06, 164.46. Anal. Calcd for $C_{32}H_{38}O_3$: C, 81.66; H, 8.14. Found: C, 81.37; H, 8.18.

1,1-Dimesityl-2-(*p*-(*N*,*N*-dimethylamino)benzoyloxy)-3,3-dimethyl-1-butene (1e). Reaction of 1,1-dimesityl-3,3-dimethylbuten-2-ol (1.80 g, 5.35 mmol) and sodium hydride (60% suspension in paraffin; 230 mg, 5.74 mmol) with 4-(*N*,*N*-dimethylamino)benzoyl chloride (2.16 g, 11.7 mmol) by the method described before yielded 1.12 g (2.32 mmol, 43%) of pure **1e** after chromatography (silica gel, toluene) and recrystallization from pentane as a white solid: mp 183 °C; IR (KBr) 2913, 1718, 1604, 1259 cm^{-1}; ^1H NMR δ 1.10 (s, 9 H), 1.94 (br s, 6 H), 2.03 (s, 3 H), 2.23 (s, 3 H), 2.54 (br s, 3 H), 2.85 (br s, 3 H), 3.82 (s, 3 H), 6.5−6.8 (br.m, 4 H), 6.84 (d, ^3J = 7.0 Hz, 2 H), 7.83 (d, ^3J = 7.0 Hz, 2 H); ^{13}C NMR δ 20.61, 20.81, 28.68, 39.35, 40.00, 110.62, 125.55, 131.27, 133.47, 135.12, 135.27, 135.97, 138.12, 151.72, 153.04, 164.94. Anal. Calcd for $C_{33}H_{41}NO_2$: C, 81.94; H, 8.54; N, 2.90. Found: C, 81.59; H, 8.75; N, 2.65.

1,1-Dimesityl-2-(ferrocenoyloxy)-3,3-dimethyl-1-butene (1f). Reaction of 1,1-dimesityl-3,3-dimethylbuten-2-ol (1.80 g, 5.35 mmol) and sodium hydride (60% suspension in paraffin; 230 mg, 5.74 mmol) with ferrocenoyl chloride (2.16 g, 11.7 mmol) by the method described above yielded 910 mg (1.66 mmol, 31%) of pure **1f** after chromatography (silica gel, toluene) and recrystallization from pentane as a brown solid: mp 110 °C; IR (KBr) 2959, 1728, 1609, 1454 cm^{-1}; ^1H NMR δ 1.05 (s, 9 H), 1.89 (br s, 3 H), 1.99 (br s, 3 H), 2.11 (s, 3 H), 2.23 (s, 3 H), 2.58 (br s, 3 H), 2.83 (br s, 3 H), 3.85 (s, 5 H), 4.32 (s, 2 H), 4.61 (br s, 1 H), 4.75 (br s, 1 H), 6.73 (br.d, 4 H); ^{13}C NMR δ 21.11, 21.25, 29.24, 39.88, 70.13, 71.42, 72.56, 126.60, 129.2 (br.), 135.63, 136.46, 136.57, 138.80, 151.89, 170.04. Anal. Calcd for $C_{35}H_{40}FeO_2$: C, 76.64; H, 7.35. Found: C, 76.30; H, 7.65.

1-(*tert*-Butylaminocarbonyloxy)-2,2-dimesityl-1-phenylethene (2a). Reaction of 2,2-dimesityl-1-phenylethenol (1.00 g, 2.81 mmol) and NaH (60% suspension in paraffin; 0.40 g, 10.0 mmol) with *tert*-butylisocyanate (4.96 g, 50.1 mmol) by the method described before yielded 0.80 g (1.93 mmol, 69%) of pure **2a** as a white solid: mp 151 °C; IR (KBr) 3444, 1750, 1610 cm^{-1}; ^1H NMR δ 1.02 (s, 9 H), 1.82 (br s, 3 H), 2.01 (s, 6 H), 2.18 (s, 3 H), 2.22 (s, 3 H), 2.48 (br s, 3 H), 4.30 (s, 1 H), 6.66 (br. s, 2 H), 6.7−6.9 (br, 2 H), 7.12 (m, 2 H), 7.20 (m, 3 H); ^{13}C NMR δ 20.72, 20.81, 21.05, 21.32, 28.30, 29.85, 50.01, 127.16, 127.64, 127.92, 128.76, 129.28, 129.80, 130.40, 134.50, 134.65, 136.16, 136.38, 136.86, 138.29, 146.63, 152.84. Anal. Calcd for $C_{31}H_{37}NO_2$: C, 81.72; H, 8.18; N, 3.07. Found: C, 81.80; H, 8.08; N, 2.86.

1-(*t*-Butoxycarbonyloxy)-2,2-dimesityl-1-phenylethene (2b). Reaction of 2,2-dimesityl-1-phenylethenol (1.00 g, 2.81 mmol) and NaH (60% suspension in paraffin; 0.40 g, 10.0 mmol) with di-*tert*-butyl dicarbonate (2.20 g, 10.1 mmol) by the method described above yielded 0.94 g (2.06 mmol, 73%) of pure **2b** as a white solid: mp 141 °C; IR (KBr) 1753, 1609 cm^{-1}; ^1H NMR δ 1.16 (s, 9 H), 1.81 (br, 3 H), 2.00 (br. s, 6 H), 2.18 (s, 3 H), 2.21 (s, 3 H,), 2.46 (br, 3 H), 6.67 (br s, 2 H), 6.7−6.9 (br, 2 H), 7.14 (m, 5 H); ^{13}C NMR δ 20.75, 21.00, 27.18, 82.00, 127.27, 127.70, 128.09, 128.55, 129.30, 133.70, 135.91, 136.33, 136.58, 138.19, 138.61, 146.28, 151.68. Anal. Calcd for $C_{31}H_{36}O_3$: C, 81.54; H, 7.95. Found: C, 81.11; H, 7.79.

Bis(1,1-dimesityl-3,3-dimethylbut-1-en-2-yl)carbonate (3a) Reaction of 1,1-dimesityl-3,3-dimethylbuten-2-ol (0.80 g, 2.38 mmol) and sodium hydride (60% suspension in paraffin; 0.40 g, 10.0 mmol) with bis(trichloromethyl)carbonate (0.23 g, 0.75 mmol) by the method described before yielded 420 mg (600 μmol, 50%) of pure **3a** as a white solid: mp 148 °C; IR (KBr) 1756, 1611; ^1H NMR δ 0.56 (s, 18 H), 1.81 (s, 6 H), 1.83 (s, 6 H), 2.13 (s, 6 H), 2.18 (s, 6 H), 2.39 (s, 6 H), 2.60 (s, 6 H), 6.52 (s, 2 H), 6.57 (s, 2 H), 6.78 (s, 2 H), 6.83 (s, 2 H); ^{13}C NMR δ 20.57, 20.78, 21.63, 22.39, 27.70, 38.37, 124.85, 127.54, 128.27, 128.85, 130.34, 134.67, 135.85, 136.07, 137.61, 138.64, 139.98, 152.53; HRMS calcd for $C_{49}H_{62}O_3$ 698.4699, found 698.4697.

Bis(1,1-dimesityl-3,3-dimethylbut-1-en-2-yl)oxalate (3b) Reaction of 1,1-dimesityl-3,3-dimethylbuten-2-ol (0.80 g, 2.38 mmol) and of sodium hydride (60% suspension in paraffin; 0.40 g, 10.0 mmol) with bis(trichloromethyl)carbonate (0.30 g, 2.36 mmol) by the method described above yielded 577 mg (794 μmol, 67%) of pure **3b** as a white solid: mp 263 °C; IR (KBr) 1756, 1610; ^1H NMR δ 0.93 (s, 18 H), 1.81 (s, 6 H), 1.91 (s, 6 H), 2.12 (s, 6 H), 2.20 (s, 6 H), 2.52 (br s, 6 H), 2.66 (br s, 6 H), 6.5−6.9 (br. 8 H); ^{13}C NMR 20.57, 20.70, 20−22 (br), 28.07, 38.50, 125.98, 127−130 (br), 133.83, 133.95, 135.98, 136.41, 137−139 (br), 155.03, 198.44; HRMS calcd for $C_{50}H_{62}O_4$ 726.4648, found 726.4630.

General Procedure for the One-Electron Oxidations of the Enol Carbamates and Enol Carbonates. In a glovebox the desired amount of the one-electron oxidant and 50 μmol of the enol derivative were placed into two separate test tubes equipped with stirring rods. At a high purity argon line acetonitrile (2 mL) was added in each test tube to dissolve the reactants. The solution of the one-electron oxidant was added dropwise via syringe to the solution of the enol and the resulting mixture was stirred overnight. The mixture was quenched with 2 mL of saturated aqueous $NaHCO_3$ and diluted with 10 mL of CH_2Cl_2. The aqueous layer was extracted three times with CH_2Cl_2, the combined organic layers were washed with saturated aqueous NaCl and water and dried over Na_2SO_4. Removal of the solvent afforded the crude product. In the reactions using $[Fe(phen)_3](PF_6)_3$ as oxidant the residue was extracted with ether and filtered off to separate insoluble iron salts. Product analysis was performed by GC, GC-MS and ^1H NMR. The benzofurans were identified by comparison with data of authentic samples. For the detailed characterization of benzofurans **B1** and **B2**, see ref 25.

Cyclic Voltammetry. In a glovebox tetra(*n*-butyl)ammonium hexafluorophosphate (232 mg, 600 μmol) and the electroactive species (6 μmol) were placed into a thoroughly dried CV cell. At a high purity argon line acetonitrile or dichloromethane (6.0 mL) was added through a gastight syringe, a 1 mm platinum disk electrode as working electrode and a Pt wire counter electrode as well as an Ag reference electrode were placed into the solution. The cyclic voltammograms were recorded at various scan rates using various starting and switching potentials. For determination of the oxidation potentials ferrocene (6 μmol) was added as the internal standard. For fast scan cyclic voltammetry, 385 mg (1.00 mmol) of supporting electrolyte, 50 μmol of substrate and 5 mL of solvent were employed as described before. Fast scan cyclic voltammograms were carried out at 25 μm Au ultramicro electrodes, a Pt wire serving as counter electrode and a Ag wire as reference electrode. Cvs were recorded using a Princeton Applied Research Model 362 potentiostat with an Philips model PM 8271 XYt-recorder for scan rates <1 V s^{-1}. For fast scan cyclic voltammetry, a Hewlett-Packard Model 331A4 Function Generator was used, connected to a three-electrode potentiostat developed by C. Amatore.[47] Data were recorded by a HP 54510 A Digitizing Oscilloscope linked to a 486DX33

computer using HP data transfer program Scopelink. The ratios I_{pc}/I_{pa} were determined according to the equation of Nicholson.[48]

Digital Simulations of the Cyclic Voltammograms. The computer simulation of the redox chemistry of the examined compounds was carried out on a PC using the Crank–Nicholson technique[49] and DigiSim.[50] The simulation of a full-cycle voltammogram consisted of 1000 data points, allowing for an acceptable resolution of the cyclic voltammograms. All chemical reactions were assumed to be reversible except the ET equilibria. With a standard heterogeneous electron-transfer constant of $k^0_{hetero} = 1$ cm·s^{-1} and standard diffusion coefficients of $D = 10^{-5}$ cm^2·s^{-1}, the rate constants for the chemical reaction steps were varied to achieve the best possible agreement with the experimental curves.

EPR. Radical cations were generated by reaction of dioxygenyl hexafluoroarsenate with the neutral compound in degassed chlorodifluoromethane at 150 K at a high vacuum line. The mixture was degassed at $<10^{-5}$ mbar and poured into a test tube, which was sealed off. The EPR spectra were recorded on a Bruker ESP300 EPR spectrometer.

Acknowledgment. We gratefully acknowledge financial support by the Deutsche Forschungsgemeinschaft (SFB 347 and Schwerpunkt "Radikale in der enzymatischen Katalyse). In addition, we are most indebted to the Fonds der Chemischen Industrie for the continuous support for our research. We thank the Degussa for a generous gift of electrode materials.

Supporting Information Available: Details of digital simulation of cyclic voltammograms and crystallographic information files are available free of charge via the Internet at http://pubs.acs.org.

JO0057093

(47) Amatore, C.; Lefrou, C.; Pflügler, F. *J. Electroanal. Chem. Interfacial* **1989**, *270*, 43.

(48) Nicholson, R. S. *Anal. Chem.* **1966**, *38*, 6.

(49) (a) Lasia, A. *J. Electroanal. Chem. Interfacial Electrochem.* **1983**, *146*, 397. (b) Heinze, J.; Störzbach, M.; Mortensen, J. *J. Electroanal. Chem. Interfacial Electrochem.* **1984**, *165*, 61. (c) Heinze, J.; Störzbach, M. *J. Electroanal. Chem. Interfacial Electrochem.* **1993**, *346*, 1.

(50) (a) Rudolph, M.; Reddy, D. P.; Feldberg, S. W. *Anal. Chem.* **1994**, *66*, 589A. (b) Rudolph, M. *J. Electroanal. Chem. Interfacial Electrochem.* **1992**, *338*, 86.